PRELIMINARY STOCK ASSESSMENT OF SOUTH ATLANTIC SWORDFISH (*XIPHIAS GLADIUS*) USING STOCK SYNTHESIS MODEL

B. Mourato[1], E. Kikuchi[2], L.G.Cardoso[2], R. Sant'Ana[3], D. Parker[4]

SUMMARY

We first attempted to apply the Stock Synthesis model for South Atlantic swordfish with the best available data through 2020. Results suggest reasonably robust fits to the data as judged by the presented model diagnostic results. The resulting stock status for 2020 was generally consistent and predicted with high probabilities that current fishing levels are sufficiently high to preclude rebuilding ($F > F_{MSY}$), whereas biomass remains below sustainable levels that can produce MSY ($SSB < SSB_{MSY}$). As such, our models conclusively estimate that stock is overfished and subject to overfishing, with probability ranging from 76.8% - 97.3% for the red quadrant of Kobe. Sensitivities analysis for important life-history parameters (such as natural mortality and steepness) showed high uncertainty regarding the stock's productivity. Research should prioritize estimating these important biological parameters to improve the parametrization of integrated age-structured models for the following assessments of South Atlantic swordfish.

RÉSUMÉ

Nous avons d'abord tenté d'appliquer le modèle Stock Synthesis à l'espadon de l'Atlantique Sud avec les meilleures données disponibles jusqu'en 2020. Les résultats suggèrent des ajustements raisonnablement robustes aux données, comme en témoignent les résultats de diagnostic du modèle présentés. L'état du stock obtenu pour 2020 était généralement cohérent et prédisait avec des probabilités élevées que les niveaux de pêche actuels élevés empêchent le rétablissement ($F > F_{PME}$), tandis que la biomasse reste en dessous des niveaux durables qui peuvent produire la PME ($SSB < SSB_{PME}$). Ainsi, nos modèles estiment de manière concluante que le stock est surpêché et victime de surpêche, avec une probabilité allant de 76,8% à 97,3% de se situer dans le quadrant rouge de Kobe. L'analyse des sensibilités pour les paramètres importants du cycle de vie (tels que la mortalité naturelle et la pente) a montré une grande incertitude concernant la productivité du stock. La recherche devrait donner la priorité à l'estimation de ces paramètres biologiques importants afin d'améliorer la paramétrisation des modèles intégrés structurés par âge pour les prochaines évaluations de l'espadon de l'Atlantique Sud.

RESUMEN

Primero intentamos aplicar el modelo Stock Synthesis para el pez espada del Atlántico sur con los mejores datos disponibles hasta 2020. Los resultados sugieren un ajuste razonablemente sólido a los datos, según los resultados de diagnóstico del modelo presentados. El estado del stock resultante para 2020 fue generalmente coherente y predijo con altas probabilidades que los niveles de pesca actuales son lo suficientemente elevados como para impedir la recuperación ($F > F_{RMS}$), mientras que la biomasa permanece por debajo de los niveles sostenibles que pueden producir el RMS ($SSB < SSB_{RMS}$). Así, nuestros modelos estiman de forma concluyente que el stock está sobrepescado y es objeto de sobrepesca, con una probabilidad que oscila entre el 76,8 % y el 97,3 % de situarse en el cuadrante rojo del diagrama de Kobe. El análisis de sensibilidades para parámetros importantes del ciclo vital (como la mortalidad natural y la inclinación) mostró una gran incertidumbre en cuanto a la productividad del stock. La investigación debería dar prioridad a la estimación de estos importantes parámetros biológicos para mejorar la

[1] Instituto do Mar, Universidade Federal de São Paulo, Av. Doutor Carvalho de Mendonça, 144, 11070-100, Santos, Brazil. E-mail: bruno.mourato@unifesp.br
[2] Laboratório de Recursos Pesqueiros Demersais, Fundação Universidade Federal do Rio Grande (FURG), Av. Itália km 8, Campus Carreiros, Rio Grande, Brazil
[3] Laboratório de Estudos Marinhos Aplicados, Escola do Mar, Ciência e Tecnologia, Universidade do Vale do Itajaí, Rua Uruguai, 458, 88302-901, Itajaí, Santa Catarina, Brazil.
[4] Department of Forestry, Fisheries and the Environment, Cape Town, South Africa

parametrización de los modelos integrados estructurados por edad para las siguientes evaluaciones del pez espada del Atlántico sur.

KEYWORDS

Billfish, stock status, age-structured model, population dynamics

1 Introduction

The Standing Committee on Research and Statistics (SCRS) of the International Commission for the Conservation of Atlantic Tunas (ICCAT) has been historically considered the existence of three distinct stocks of swordfish *(Xiphias gladius*) in the Atlantic Ocean: North Atlantic (NA), South Atlantic (SA) and the Mediterranean Sea. Historically, the SA swordifsh stock has been assessed using surplus production models (SPM), including the ASPIC, BSP2, and JABBA models. In contrast, the NA swordfish stock has been assessed using an integrated age-structured model Stock Synthesis. The last assessment in 2017 showed that BSP2 and JABBA models produced comparable results for the SA swordfish, with the stock being estimated as overfished, and overfishing was either occurring, or fishing mortality was very close to F_{MSY}, in 2015 (ICCAT, 2017; Winker et al., 2018).

Considering that SPM models may not fully capture the true dynamics (i.e., size-structure) of the SA swordfish stock, including important aspects, such as the introduction of the minimum size limit and its effects on the population, the implementation of the integrated age-structured model for the SA swordfish stock assessment is a priority (ICCAT, 2022). While available biological information is much more focused on the NA swordfish stock (Neilson et al. 2013), there is a lack of essential life-history parameters available to the South, such as age and growth studies, and for such reason, the application of age-structured models has been prevented. On the other hand, a substantial amount of size-frequency data (Kimoto et al., 2022) and CPUE indices has been available from the main fleets that operate in the South Atlantic (ICCAT, 2022).

In this sense, we attempt to apply the first integrated age-structured model Stock Synthesis for the SA swordfish with the best available data, including updated catch, CPUE, and length-composition time series through 2020. Extensive model diagnostics are provided to evaluate the model fits, retrospective patterns, and prediction skills. In addition, this preliminary assessment of the SA swordfish also included several assumptions for the model structure and the inputting life-history parameters. Therefore, our preliminary results might guide the discussion of the axes of uncertainty for the main parameters and priorities for the data collection and biological research to improve the future stock assessments.

2 Methods

2.1 Fleet structure and fisheries data

Based on data presented at the 2022 Swordfish Data Preparatory Meeting (ICCAT, 2022), the Stock Synthesis model was parametrized using 12 different fishing fleets (**Figure 1**, **Table 1**). The longline fisheries were Spain, Brazil, Japan early, Japan late, Chinese Taipei early, Chinese Taipei late, South Africa, Uruguay, Portugal, "Others longline" and "Others with multiple fishing gears". The Spanish, Japanese and Chinese Taipei indices were all split into two separate time blocks as discussed in the data preparatory meeting (ICCAT, 2022). The total catch, from 1950 to 2020, including reported landings and dead discards were calculated by the ICCAT Secretariat (**Figure 2**), and was assumed to be known essentially with a CV of 0.01 in the model. Standardized CPUE series were obtained from several major fishing fleets operating in the South Atlantic, all of which were longline (LL), including Brazil, EU-Spain, Japan, Uruguay, Chinese Taipei and South Africa (**Figure 3**). For the length composition data, the information was compiled by the ICCAT secretariat which covered most of the fishing fleets operating in the South Atlantic (**Figure 4**). Length composition data (lower jaw fork length, LJFL) were modeled assuming a multinomial distribution with 5 cm length bins (20-435 range). The effective sample sizes were equal to the *ln* (number of observations), to reduce the effect of pseudo-replication in sampling and decrease the weight of length data in the overall model likelihood.

2.2 Life-history parameters

The main life-history parameters are depicted in **Table 2**. Size at 50% maturity was set at 156 cm LJFL for females, and 125 cm LJFL, for males (Hazin et al., 2002). The size at fully mature was set at 180 and 149 cm LJFL for females and males, respectively. Growth parameters for both sexes were obtained in Garcia et al. (2016), while the maximum age was set at 25 years. Natural mortality for both sexes was fixed at 0.20 per age (**Table 2**). Fecundity was modeled as female stock spawning biomass (SSB) (i.e., weight-at-age multiplied by the maturity ogive) and proportional to length (eggs=a*Lb), with the length-weight relationship was used to convert the size to weight (see parameters in **Table 2**, Forselledo et al., 2017).

2.3 Model parametrization

Model was parametrized with one-area, two-sex, yearly using version 3.30.18 with a temporal domain of 1950-2020. A standard Beverton-Holt stock recruit relationship was assumed with steepness and sigmaR being fixed at 0.7 and 0.4. The equilibrium recruitment (R0) was estimated without a prior. The deviations from the stock-recruitment relationship were assumed to follow a lognormal distribution estimated on a log scale as $N(0, \text{sigmaR})$ variates with a minimum and maximum of -5 and 5, respectively. Zero recruitment deviations were assumed until the start of informative data on size structure (continuous length composition series from the main fleets), i.e., annual deviates were only estimated from 1991 to 2017. Adjustment of bias correction on recruitment was set using the *r4ss* R package tunning suggestion. The Dirichlet-multinomial likelihood was applied for data-weighting for length composition data and an "additive variance" parameter were added to each CPUE.

Selectivity was parameterized as length-based for all fleets, with the model freely estimating the selectivity parameters. Two models were considered, for the “Sel_Asym_model”, it was assumed to be an asymptotic shape for all fleets. However, the exploratory analysis indicated a poor length composition fit for some fleets. For such reason, we also explored an alternative model (“Sel_DN model”), with the same parameters as the “Sel_Asym_model”, except for the selectivity shapes of the fleets from Brazil, Spanish (first period), Japanese (first period), and Chinese-Taipei (two periods), which was set to be dome-shaped.

2.4 Model Diagnostics

Model diagnostics were assessed using the Carvalho et al. (2021) flow chart, using the R packages *ss3diags* and *r4ss* (Taylor et al., 2021; Winker et al., 2022), and included the following steps:

1) checking the hessian matrix.
2) a residual analysis of CPUE and length composition fits.
3) a retrospective analysis with eight-year retrospective peels.
4) a model’s prediction skill evaluation by applying a hindcasting cross-validation technique.
5) a likelihood profile evaluation of critical parameters (steepness, R0, and M).

3 Results and Discussion

Overall, the model showed relatively good diagnostic performance, showing good convergence properties and run in about 7 minutes. The final gradient of model was 0.000205326, and the Hessian matrix for the parameter estimates was positive definite. The total log-likelihood R0 profile seems to be consistent between the length-composition and the indices data, with the length-composition gradient being more significant than other data sources and attaining a minimum at levels close to the minimum achieved in the log-likelihood profile for the CPUE indices (**Figure 5**). Changes in log-likelihood for the length-composition by fleet showed consistency concerning the minimum value along the R0 profile among data sources. In contrast, the minimum log-likelihood for the indices by fleet indicated somewhat conflicting signals from multiple data sources (**Figure 5**).

The joint residual plots showed a random pattern for the residuals of the fits to the index for all fleets with a RMSE of 22.6% and 21.6%, for the “Sel_Asym_model” and “Sel_DN model”, respectively (**Figure 6, Figure 7**), with the longline fleets from Uruguay and Japan late seems to be the most influential and exhibited the highest discrepancies between CPUE series and model predictions (**Figure 6** and **Figure 7**). The results of the log-residuals runs test for each CPUE fit by year and model are provided in (**Figure 7**)**.** The CPUE time series from SPNLL (1st period), JPNLL (two periods) and CTPLL (two periods) failed the runs test diagnostic procedure. The reason for failing the runs tests is probably related to data-conflicts caused by the opposite trends compared to the other CPUE time series, but also by the presence of an extreme values.

Overall, the length composition data reasonably fit with few systematic departures the "Sel_Asym_model" (**Figure 8**). However, the size composition of the SPNLL early, JPNLL early, CTPLL early, CTPLL late and BRALL presented some discrepancies across the bin sizes higher than 200 cm LJFL. In contrast, the "Sel_DN model" provided a better fit to the observed length composition data (**Figure 9**). In fact, the joint residual plots and runs tests of the length composition fits also showed an improvement fits for the the "Sel_DN model" (**Figure 8** and **Figure 9**). Estimated selectivity at length are depicted in **Figure 10.** The "Sel_Asym_model" model has an asymptotic selectivity for all fleets and capture much larger fish, which help to explain the discrepancies across the bin sizes higher than 200 cm LJFL (**Figure 8**). On the other hand, the doming of the SPNLL1, JPNLL, CTPLL, and BRALL is steep with lower probability to capture larger fish and follows these fleets' size composition (**Figure 10**).

Overall, the recruitment deviations time series show a highly variable pattern around zero, but with a decreasing trend from 2014 to 2018 (**Figure 11**). The estimated stock-recruitment relationship indicates that higher recruitments are associated with low SSB levels. In contrast, low recruitment events are related to high SSB levels but are associated with high interannual variability in estimated recruitment deviations (**Figure 11**). For both models, the trajectory of SSB/SSB_{MSY} presented similar trends and showed a sharp decrease from the mid-1960s to an overfished status until the final of the 2000s, followed by a stable trend but remained at levels below SSB_{MSY} to 2020 (**Figure 12**). The F/F_{MSY} trajectory showed an overall increasing trend from the beginning of the time series to an overfishing status after the final 1980s, reaching its high value in the mid-2000s. Afterward, fishing mortality was characterized by a decreasing trend until the mid-2010s, but it remained above F_{MSY} and even increased slightly toward 2020 (**Figure 12**).

The results of an eight-year retrospective analysis applied to both models are depicted in **Figure 13** and show a negligible retrospective pattern for both models. The estimated Mohn's rho for SSB and F/F_{MSY} fell within the acceptable range of -0.15 and 0.20 (Hurtado-Ferro et al., 2014; Carvalho et al., 2017) and confirmed the absence of an undesirable retrospective pattern. Hindcasting cross-validation results suggest that only CTPLL2 and ZAFLL have good prediction skills as judged by the MASE scores of approximately lower than one **(Figure 14**), albeit the MASE score for BRALL was slightly higher than one. The worst indices were SPNLL and JPNLL2. Overall, the MASE scores for the alternative model (Sel_DN model) presented a slight improvement in relation to the base case model (**Figure 14**). The sensitivity runs were conducted to evaluate different parameter combinations for the natural mortality and steepness (**Figure 15**). Depending on the assumptions of natural mortality and steepness, the stock may have reached an overfished status or may have an ongoing overfishing. Overall, lower steepness and natural mortality values resulted in smaller SSB and high fishing mortality at the end of the time series (**Figure 15**).

Summaries of parameters and benchmarks are presented in **Table 3.** Yield curves presented similar shapes achieving its maximum level around 0.27 of SSB_0, with estimates of *MSY* of 9,560 t for the "Sel_Asym_model" and 10,442 t for the "Sel_DN_model" (**Table 3**, **Figure 16**). The resulting stock status for 2020 for both models are consistent and indicated that the stock is overfished ($B_{2020} < B_{MSY}$ **Table 3**) and overfishing is occurring ($F_{2020} > F_{MSY}$ **Table 3**) which preclude the stock rebuilding, whereas biomass remains below sustainable levels that can produce MSY. Kobe biplots show the typically anti-clockwise pattern with the stock status moving from underexploited through a period of unsustainable fishing to the overexploited phase (**Figure 17**). The resulting stock status for 2020 were generally consistent and predicted with high probabilities that current fishing levels are sufficiently high to preclude rebuilding ($F > F_{MSY}$), whereas biomass remains below sustainable levels that can produce *MSY* ($B < B_{MSY}$). All models indicate that the current stock status is in the red quadrant of the Kobe biplot ($B_{2020}<B_{MSY}$ and $F_{2020}>F_{MSY}$; **Table 3**) with probability ranging from 76.8% - 97.3%, however it was noted that the "Sel_DN_model" is more optimistic regarding stock status. As such, all models conclusively estimate that stock is overfished and subject to overfishing (**Figure 17**).

Our results suggest that both models provide reasonably robust fits to the data as judged by the presented model diagnostic results. Both models performed very similarly regarding the residual's diagnostics, with a slight improvement in this regard for the "Sel_DN_model". Also, it is essential to note that there is a considerable lack of basic life history information for the SA swordfish, including the growth parameters and steepness, making it even more important to admit uncertainty about the stock's productivity. Sensitivities for the natural mortality assumption were also an important parameter for determining stock status for SA swordfish. Research should be prioritized on estimating these important biological parameters to improve the parametrization of integrated age-structured models for the following assessments of SA swordfish.

4 Acknowledgements

The authors would like to thank the ICCAT Secretariat for preparing the input data used in this analysis.

5 References

Anhøj, J., Olesen, A.V., 2014. Run charts revisited: A simulation study of run chart rules for detection of non-random variation in health care processes. PLoS One 9, 1–13.

Carvalho, F., Winker, H., Courtney, D., Kapur, M., Kell, L., Cardinale, M., ... & Methot, R. D. 2021. A cookbook for using model diagnostics in integrated stock assessments. Fisheries Research, 240, 105959.

Carvalho, F., Punt, A.E., Chang, Y.J., Maunder, M.N., Piner, K.R., 2017. Can diagnostic tests help identify model misspecification in integrated stock assessments? Fish. Res. 192, 28–40.

Forselledo, R., Mas, F., Ortiz, M. and Domingo, A. 2017. Length-Length and Length-Weight relationships ofswordfish, Xiphias gladius, caught by longliners in the Southwestern Atlantic Ocean. Collect. Vol. Sci.Pap. ICCAT, 74(3): 1151-1157

Garcia, A; Tserpes, G. and Santos, M.N. 2016. Validation of annulus formation and growth estimation of South Atlantic swordfish. Journal of the Marine Biological Association of the United Kingdom, 97: 1511-1518.

Hazin, F. H. V., H. G. Hazin, C. E. Boeckmann, P. Travassos. 2002. Preliminary study on the reproductive biology of swordfish, *Xiphias gladius* (Linnaeus 1758), in the southwestern equatorial Atlantic Ocean. Collect. Vol. Sci. Pap. ICCAT, 54(5): 1560-1569.

Hurtado-Ferro, F., Szuwalski, C.S., Valero, J.L., Anderson, S.C., Cunningham, C.J., Johnson, K.F., Licandeo, R., McGilliard, C.R., Monnahan, C.C., Muradian, M.L., Ono, K., Vert-Pre, K.A., Whitten, A.R., Punt, A.E., 2014. Looking in the rear-view mirror: Bias and retrospective patterns in integrated, age-structured stock assessment models, in: ICES Journal of Marine Science. pp. 99–110.

ICCAT, 2022. Report of the 2022 ICCAT Atlantic swordfish data preparatory session. 75p.

ICCAT, 2017. Report of the 2017 ICCAT Atlantic swordfish stock assessment session. Collect. Vol. Sci. Pap. ICCAT 74, 841–967.

Kimoto, A.; Ortiz, M and Taylor, N. 2022. Review of the fleet structure for the stock synthesis assessment models for the north and south Atlantic swordfish stocks. Collect. Vol. Sci. Pap. ICCAT, 79(2): 134-155

Methot Jr, R. D. and Wetzel, C. R. 2013. Stock synthesis: a biological and statistical framework for fish stock assessment and fishery management. Fisheries Research, 142, 86-99.

Neilson, J., Arocha, F., Cass-Calay, S., Mejuto, J., Ortiz, M., Scott, G., Smith, C., Travassos, P., Tserpes, G., Andrushchenko, I., 2013. The Recovery of Atlantic Swordfish: The Comparative Roles of the Regional Fisheries Management Organization and Species Biology. Rev. Fish. Sci. 21, 59–97.

Taylor, I.G., Doering, K.L., Johnson, K.F., Wetzel, C.R., Stewart, I.J., 2021. Beyond visualizing catch-at-age models: Lessons learned from the r4ss package about software to support stock assessments. Fisheries Research, 239:105924

Winker, H.; Carvalho, F.; Cardinale, M. and Kell, L. 2022. ss3diags: What the Package Does (OneLine, Title Case). R package version 1.0.9.

Winker, H., Carvalho, F., Kapur, M., 2018. JABBA: Just Another Bayesian Biomass Assessment. Fish. Res. 204, 275–288. https://doi.org/http://doi.org/10.1016/j.fishres.2018.03.01

Table 1. Fleet structure for the South Atlantic swordfish SS3 model.

Fleet	Fishery ID	Description	Time	Flag Name	Gear	CPUE
1	SPNLL1	EU-Spain LL	1950-2020	EU-Espana	LL	1989-1999
2	SPNLL2	EU-Spain LL	1950-2020	EU-Espana	LL	2000-2019
3	BRALL	Brazil LL	1950-2020	Brazil	LL	1994-2020
4	JPNLL1	Japan LL early	1950-1993	Japan	LL	1976-1993
5	JPNLL2	Japan LL late	1994-2020	Japan	LL	1994-2020
6	CTPLL1	Chinese Taipei LL early	1950-1990	Chinese Taipei	LL	1968-1990
7	CTPLL2	Chinese Taipei LL late	1991-2020	Chinese Taipei	LL	1997-2020
8	ZAFLL	South Africa LL	1950-2020	South Africa	LL	2004-2020
9	URYLL	Uruguay LL	1950-2013	Uruguay	LL	2001-2012
10	PORLL	Portugal LL	1950-2020	Portugal	LL	-
11	OthLL	LL by the other CPCs	1950-2020	all others	LL	-
12	Others	All others	1950-2020	all others	all	-

Table 2. Life-history parameters for the South Atlantic swordfish SS3 model.

	Females	Males	Reference
Linf	308	239	Garcia et al. (2016)
K	0.093	0.145	Garcia et al. (2016)
t0	-2.246	-1.736	Garcia et al. (2016)
a	1.69e-06	4.61e-06	Forselledo et al. (2017)
b	3.32	3.12	Forselledo et al. (2017)
L50	156	-	Hazin et al. (2002)
L100	180	-	Hazin et al. (2002)
A50	5	-	ICCAT (2017, 2022)
A100	6	-	ICCAT (2017, 2022)
M	0.2	0.2	ICCAT (2017, 2022)
MaxAge	25	25	ICCAT (2017, 2022)

Table 3. Summaries of parameters and management quantities of interest and associated the standard deviations for the South Atlantic swordfish SS3 models.

	Sel_Asym_Model		Sel_DN_Model	
	estimate	***std dev***	***estimate***	***std dev***
SSB_0	90270	4102	104495	3742
Total biomass at virgin conditions	205462	9338	237839	8517
SSB_{MSY}	24734	1142	28195	1021
F_{MSY}	0.128	0.001	0.1237	0.001
MSY	9560	415	10442	351
SSB_{MSY}/SSB_0	0.2740	0.001	0.2698	0.001
SSB_{2020}/SSB_{MSY}	0.7932	0.0873	0.8346	0.1153
F_{2020}/F_{MSY}	1.3056	0.1411	1.1435	0.1532

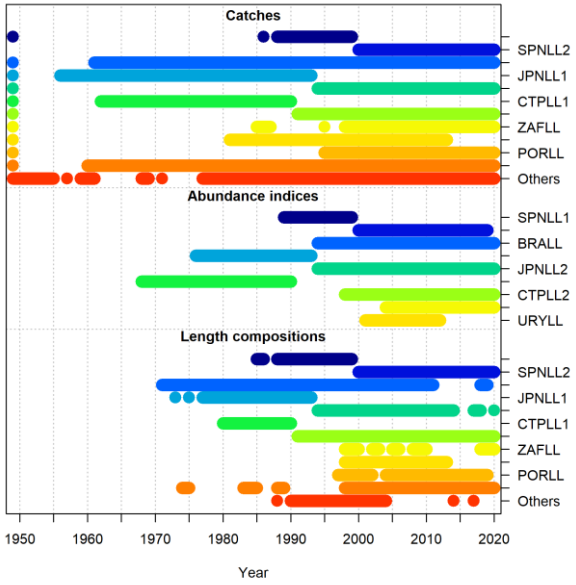

Figure 1. Data presence by year for each fleet and data type for the South Atlantic swordfish SS3 model.

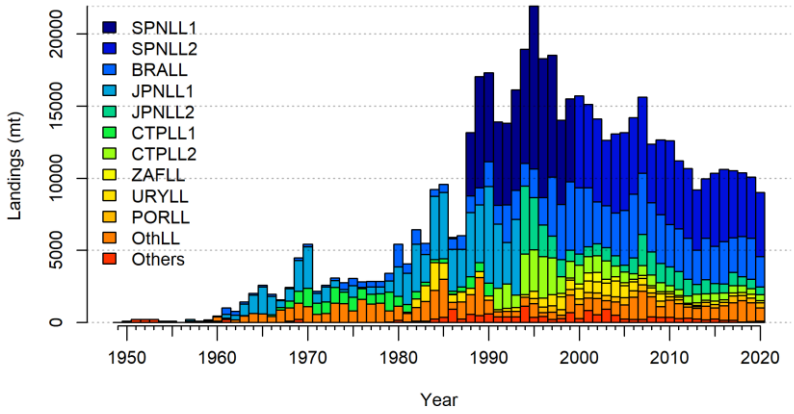

Figure 2. Task I landings input for the South Atlantic swordfish SS3 model.

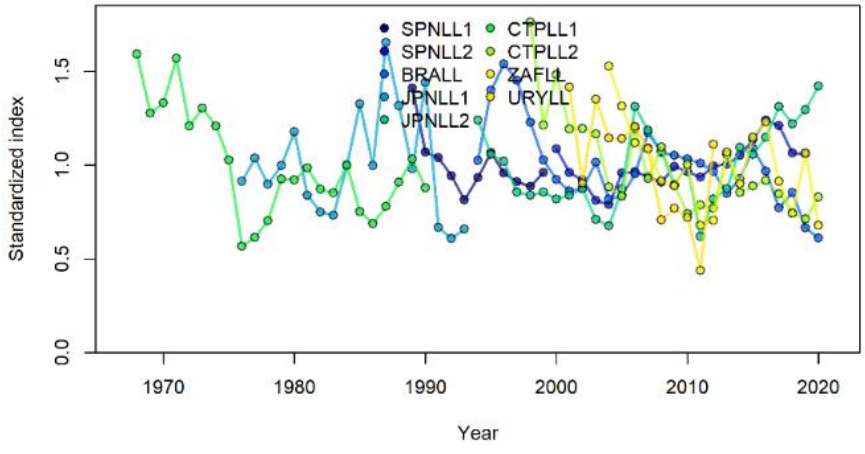

Figure 3. Standardized indices for the South Atlantic swordfish SS3 model.

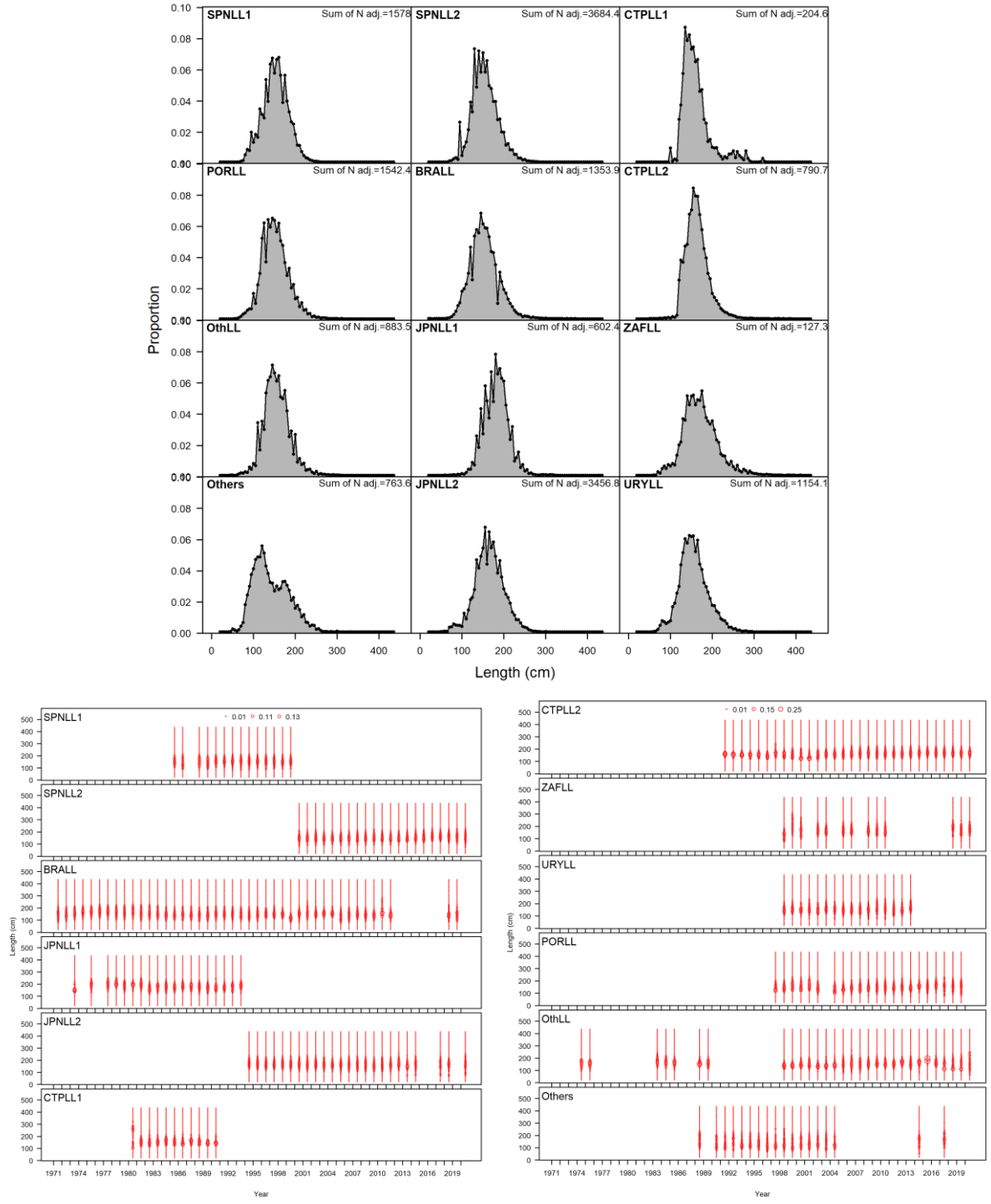

Figure 4. Length composition data input for the South Atlantic swordfish SS3 model.

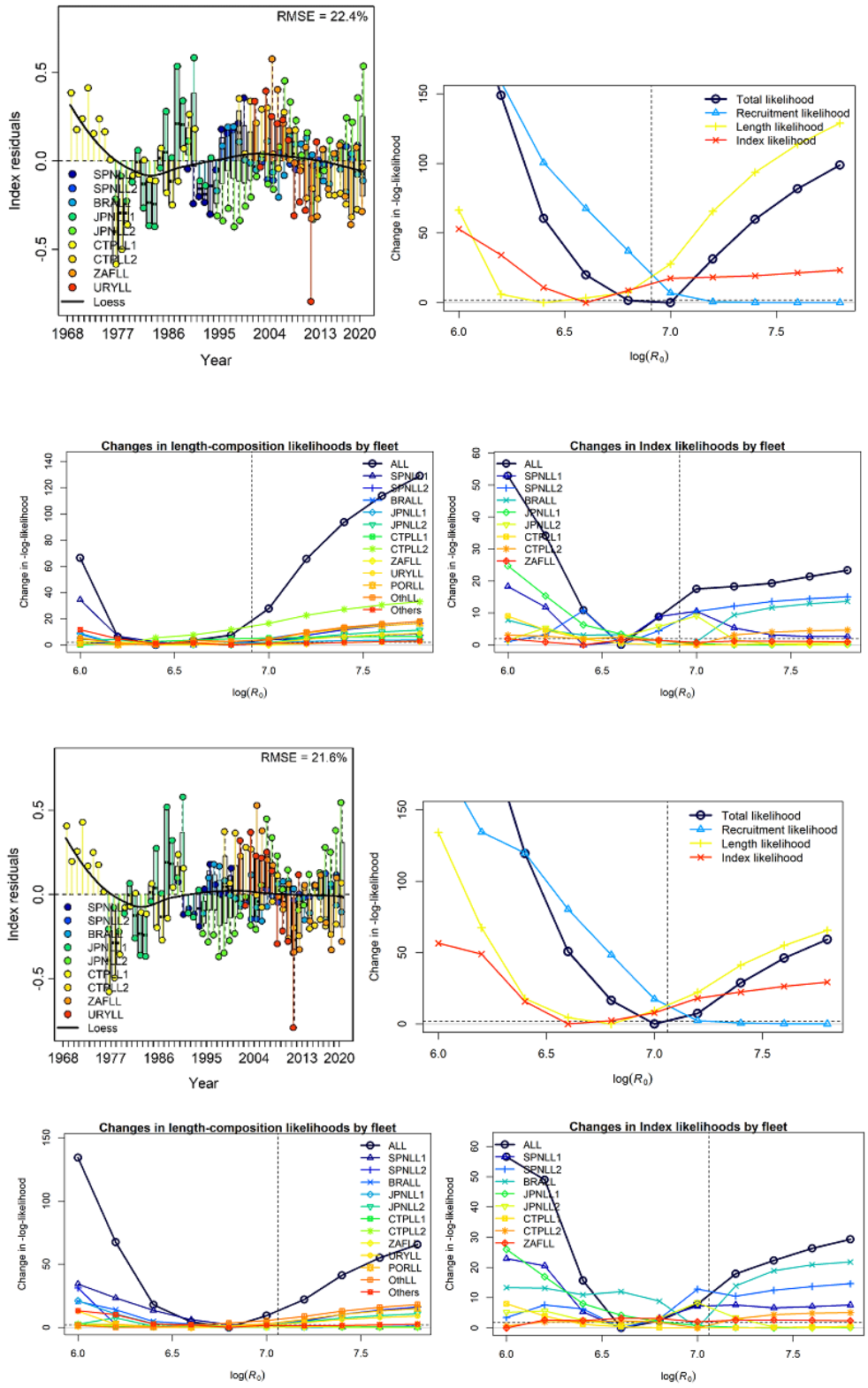

Figure 5. Joint residuals plot for the index fits and likelihood profiles for R0 for the South Atlantic swordfish SS3 models. Upper panels ("Sel_Asym_model"): Lower panels ("Sel_DN model")

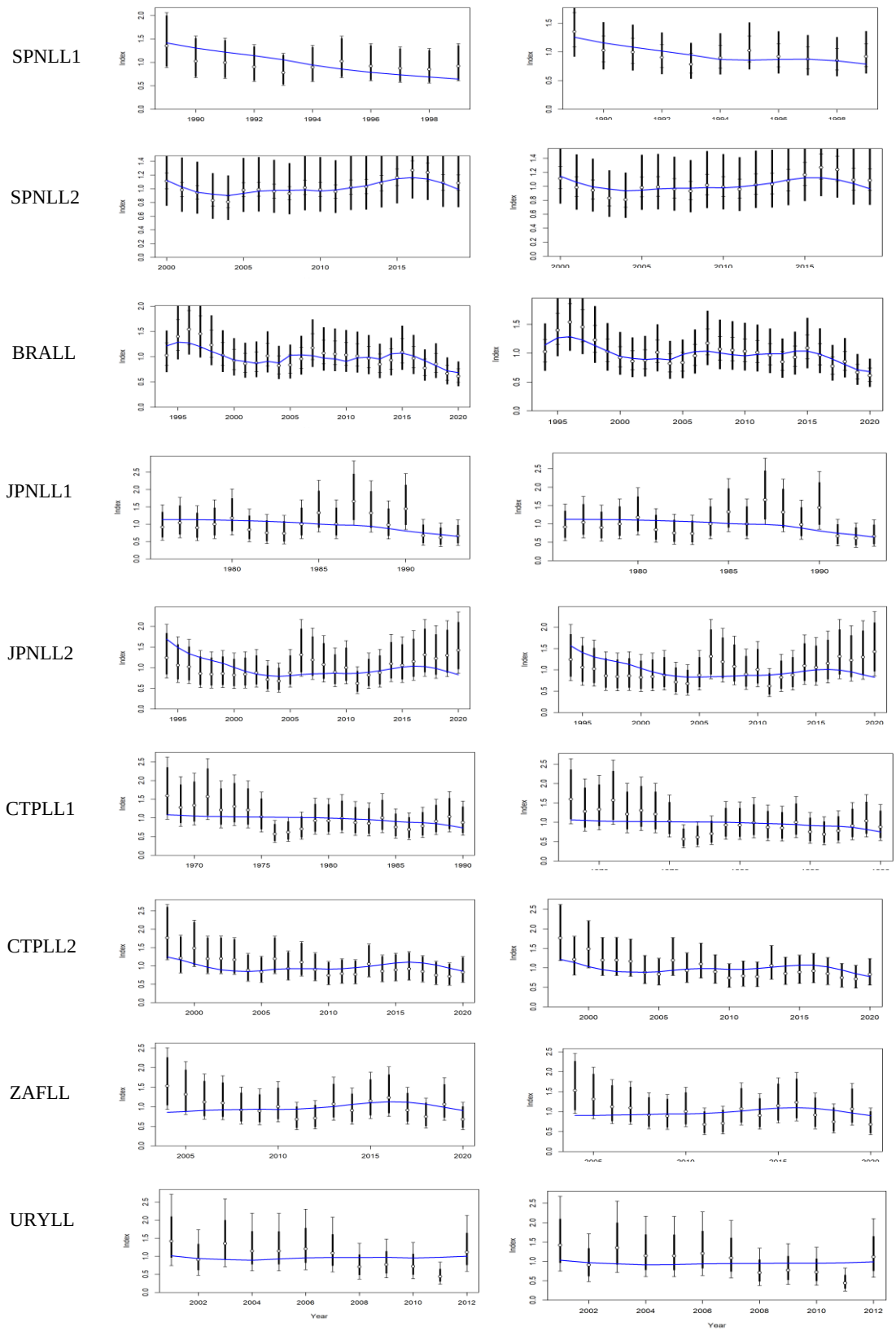

Figure 6. CPUE fits for each fleet for the South Atlantic swordfish SS3 models. Left panels ("Sel_Asym_model"); Right panels ("Sel_DN model").

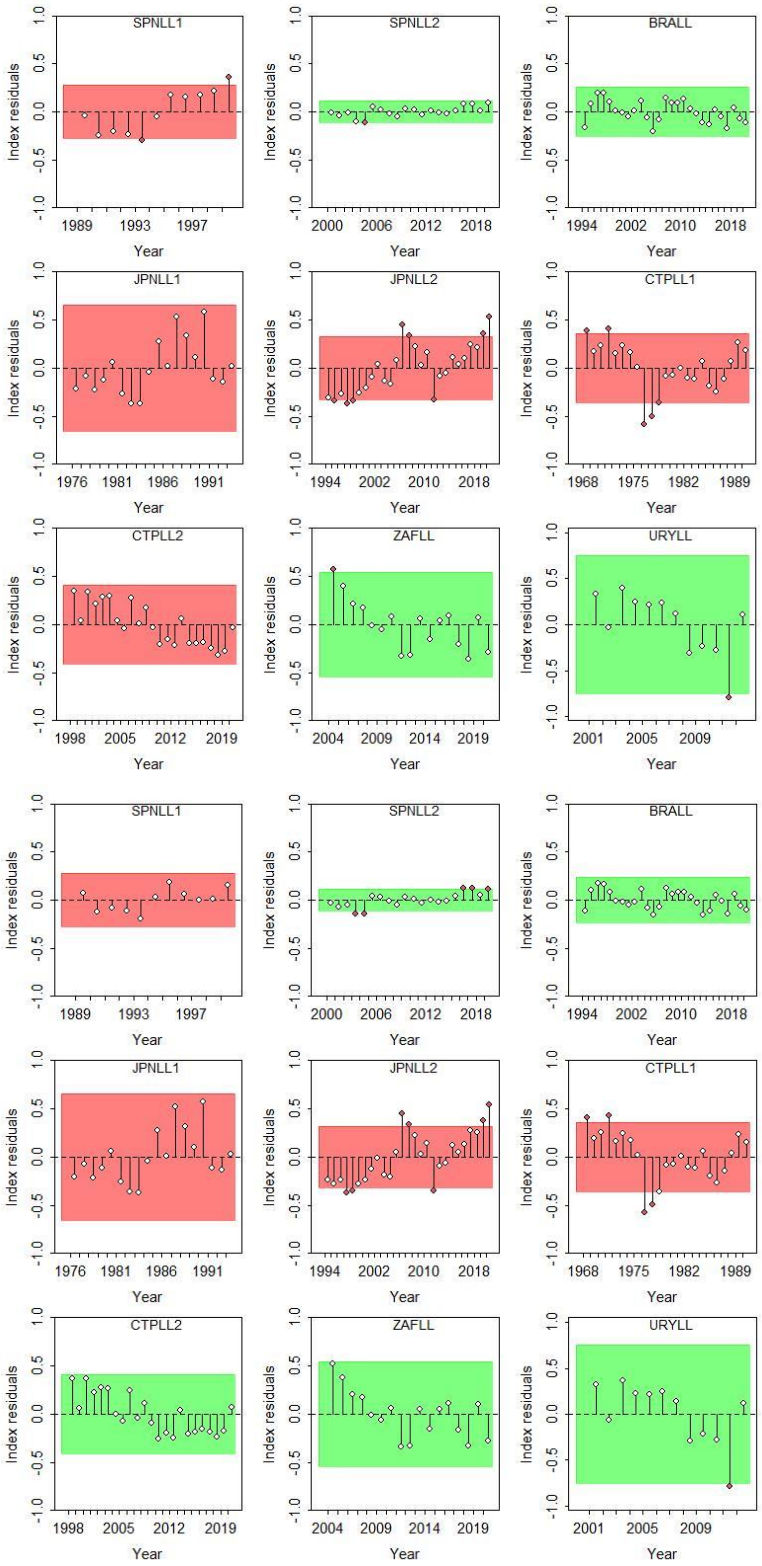

Figure 7. Runs tests to quantitatively evaluate the randomness of the time series of CPUE residuals by fleet for the base case models. Green panels indicate no evidence of lack of randomness of time-series residuals ($p>0.05$) while red panels indicate the opposite. The inner shaded area shows three standard errors from the overall mean and red circles identify a specific year with residuals greater than this threshold value (3x sigma rule). Upper panels ("Sel_Asym_model"): Lower panels ("Sel_DN model")

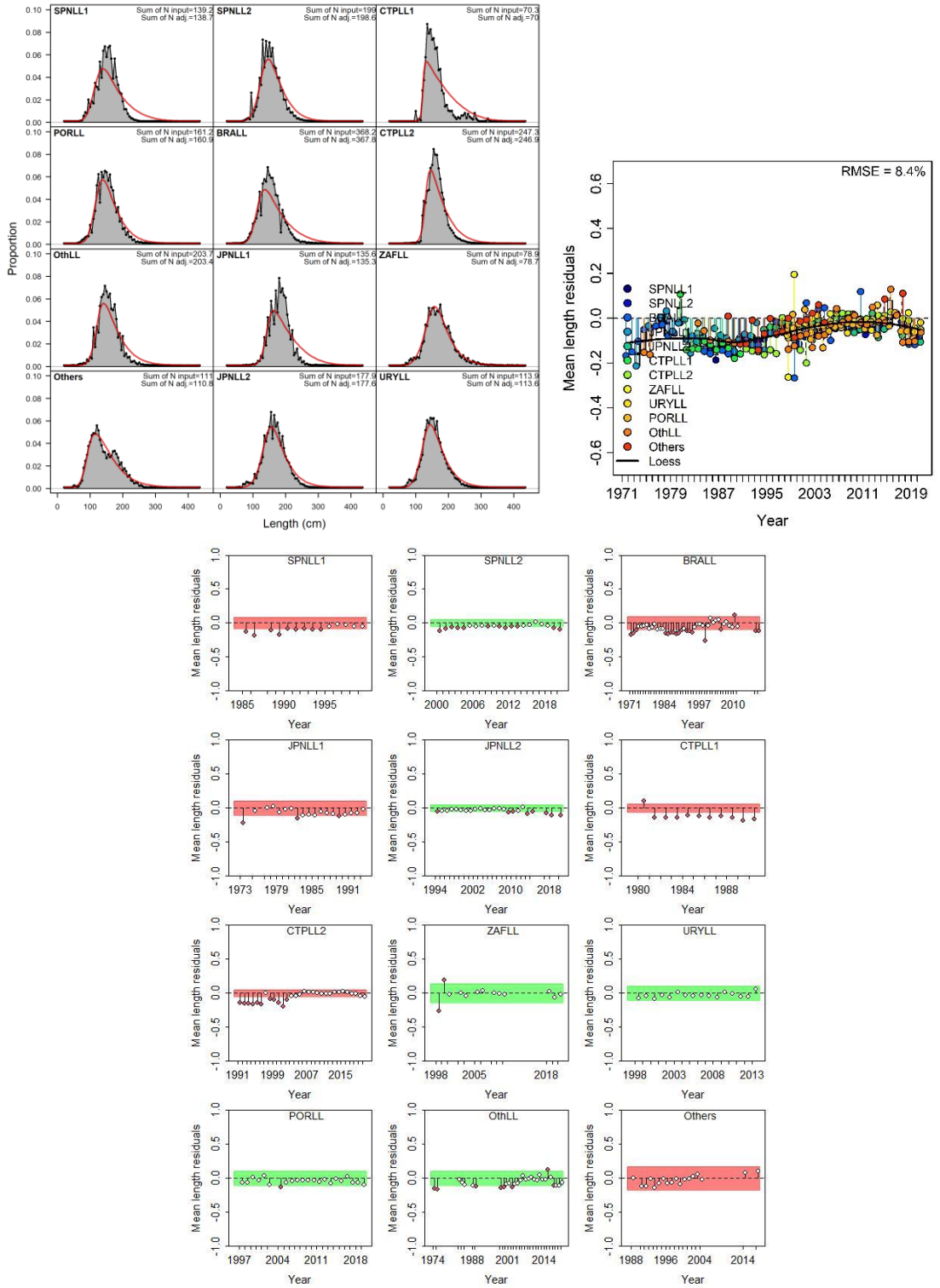

Figure 8. Model fits to the aggregated length compositions for each fleet (upper left panels), joint residuals plot for the length composition fits (upper right panel) and runs tests to length composition fits (lower panels) for the South Atlantic swordfish SS3 ("Sel_Asym_model"). Green panels indicate no evidence of lack of randomness of time-series residuals (p>0.05) while red panels indicate the opposite. The inner shaded area shows three standard errors from the overall mean and red circles identify a specific year with residuals greater than this threshold value (3x sigma rule).

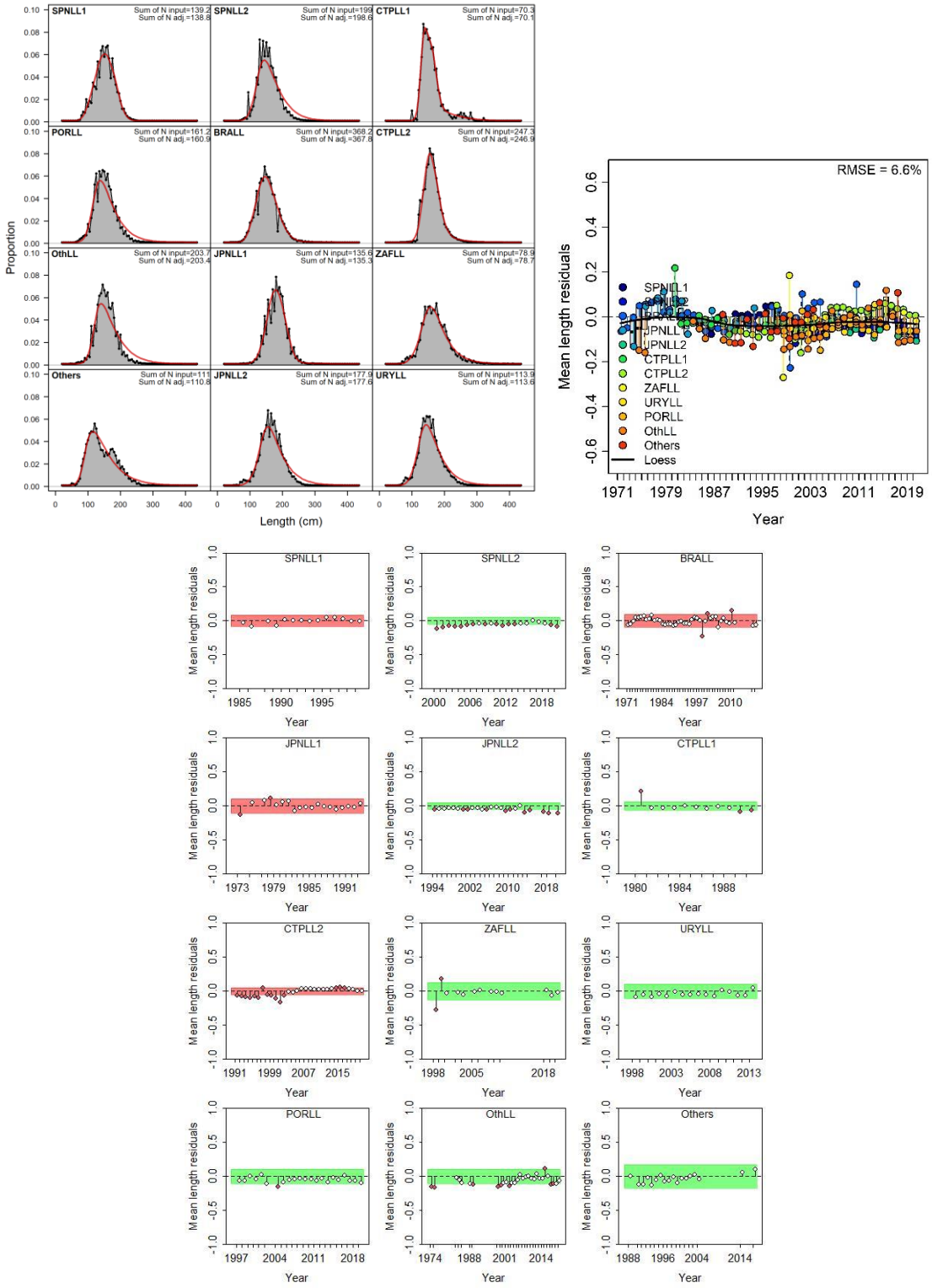

Figure 9. Model fits to the aggregated length compositions for each fleet (upper left panels), joint residuals plot for the length composition fits (upper right panel) and runs tests to length composition fits (lower panels) for the South Atlantic swordfish SS3 ("Sel_DN model"). Green panels indicate no evidence of lack of randomness of time-series residuals (p>0.05) while red panels indicate the opposite. The inner shaded area shows three standard errors from the overall mean and red circles identify a specific year with residuals greater than this threshold value (3x sigma rule).

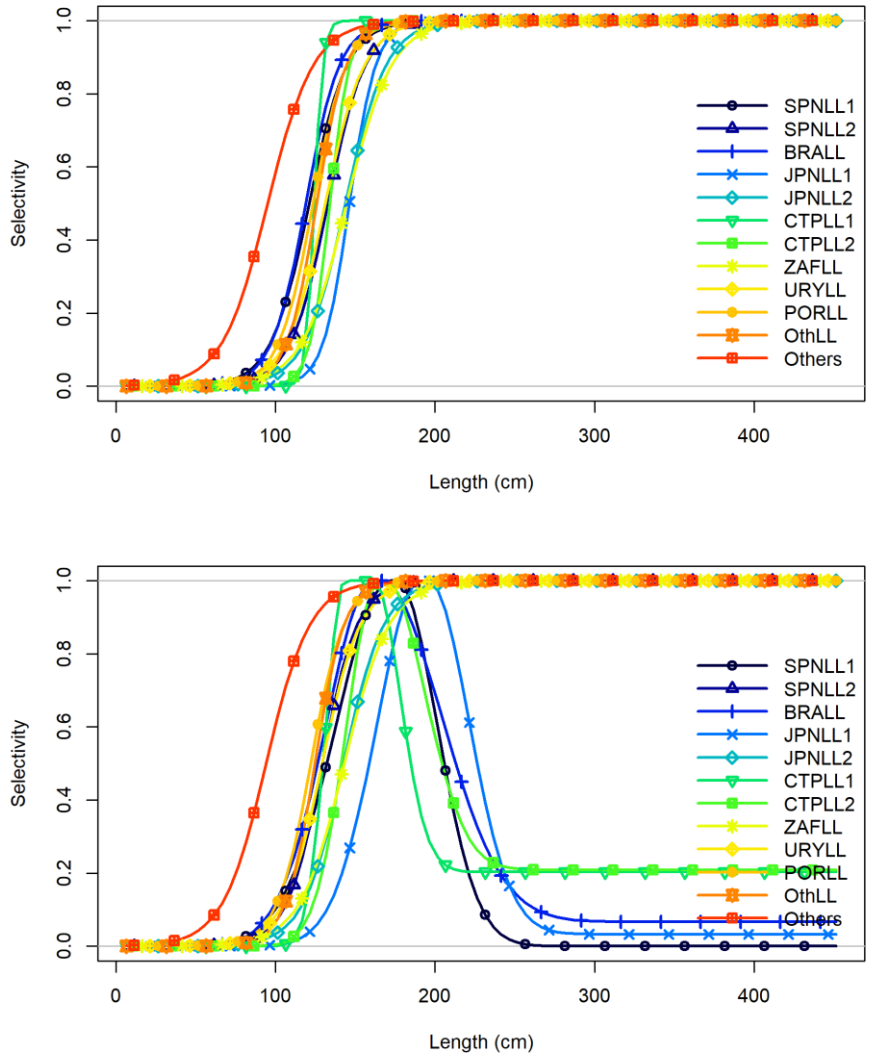

Figure 10. Selectivity at length shapes for the SS models. Upper panels ("Sel_Asym_model"): Lower panels ("Sel_DN model").

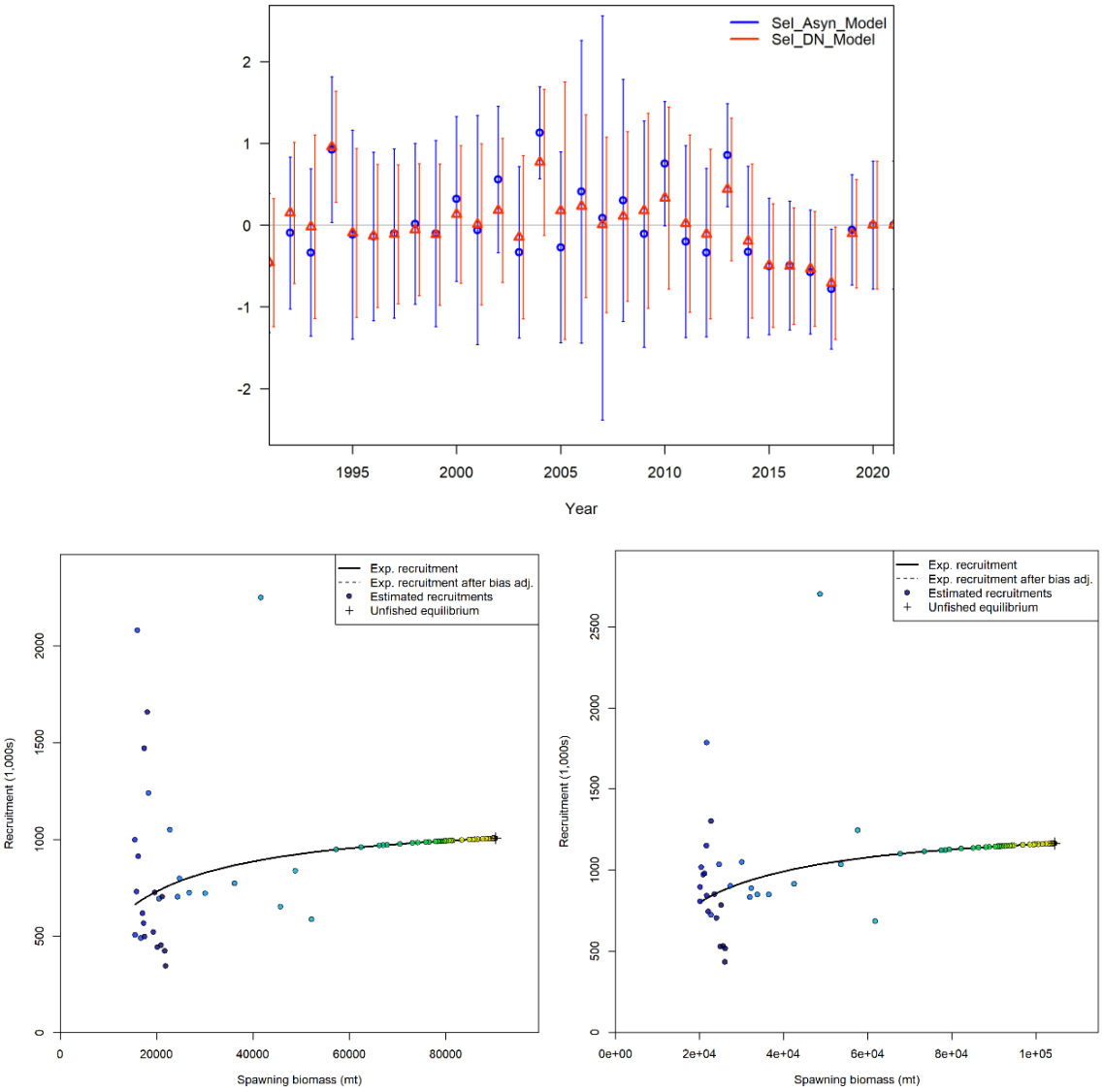

Figure 11. Recruitment deviations with 95% intervals (upper panel) and stock-recruitment curve (lower panel, left - "Sel_Asym_model"; right - "Sel_DN model"). Point colors indicate year, with warmer colors indicating earlier years and cooler colors showing later years.

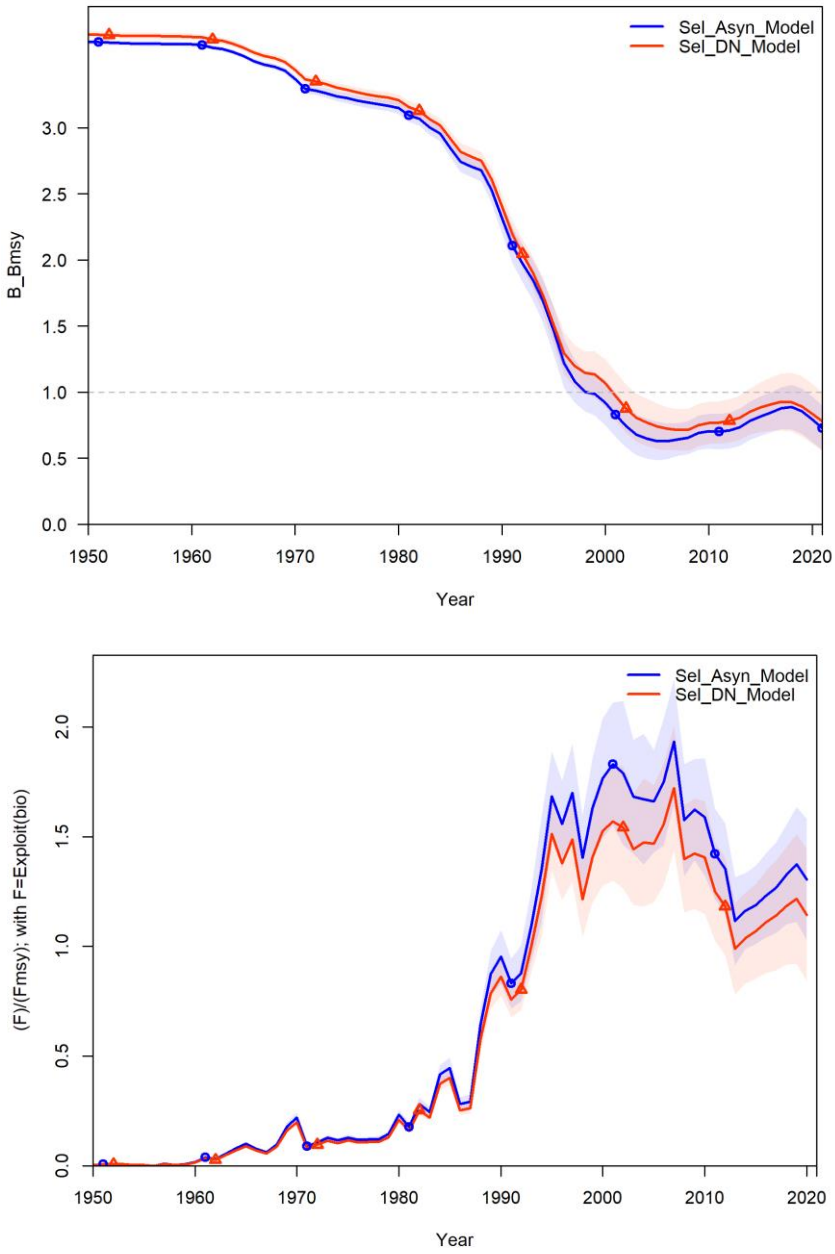

Figure 12. Trends in spawning biomass relative to SSB_{MSY} (SS$B/SSB_{MSY}$) and fishing mortality relative to F_{MSY} (F/F_{MSY}) for each model scenario from the for the South Atlantic swordfish SS3 model.

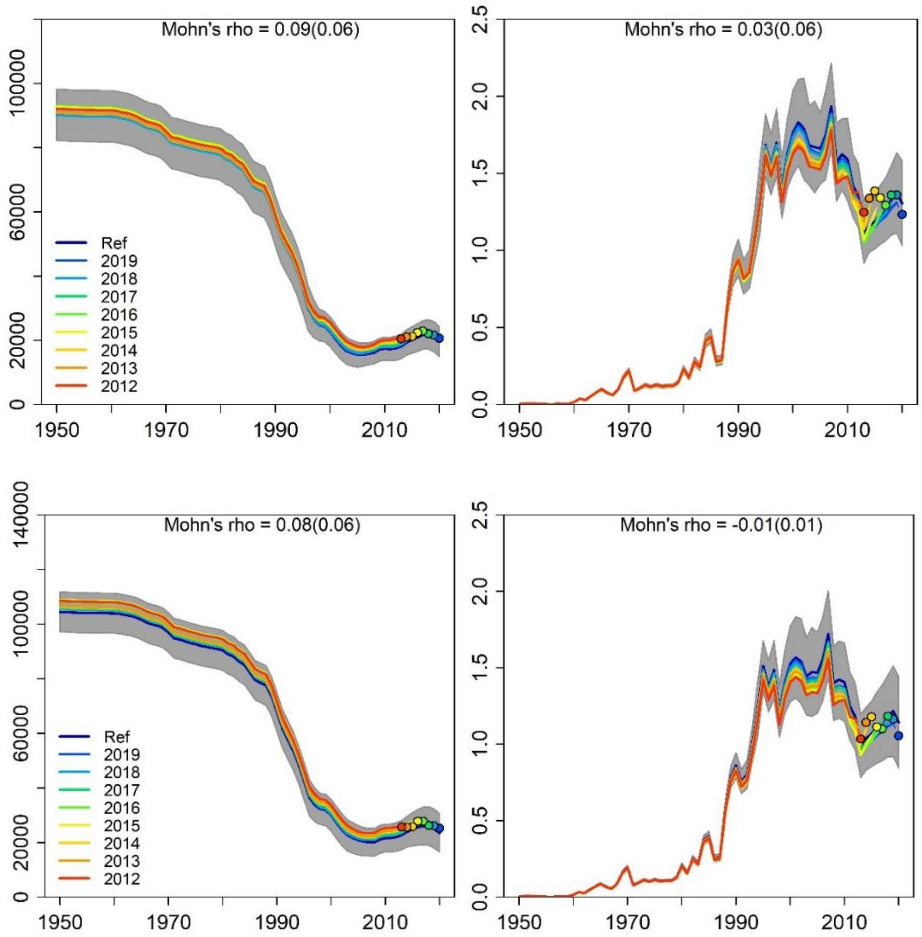

Figure 13. Retrospective analysis for the South Atlantic swordfish SS3 model, by removing one year at a time sequentially (n=8) and predicting the trends in biomass and relative fishing mortality. Upper panels ("Sel_Asym_model") and lower panels ("Sel_DN model").

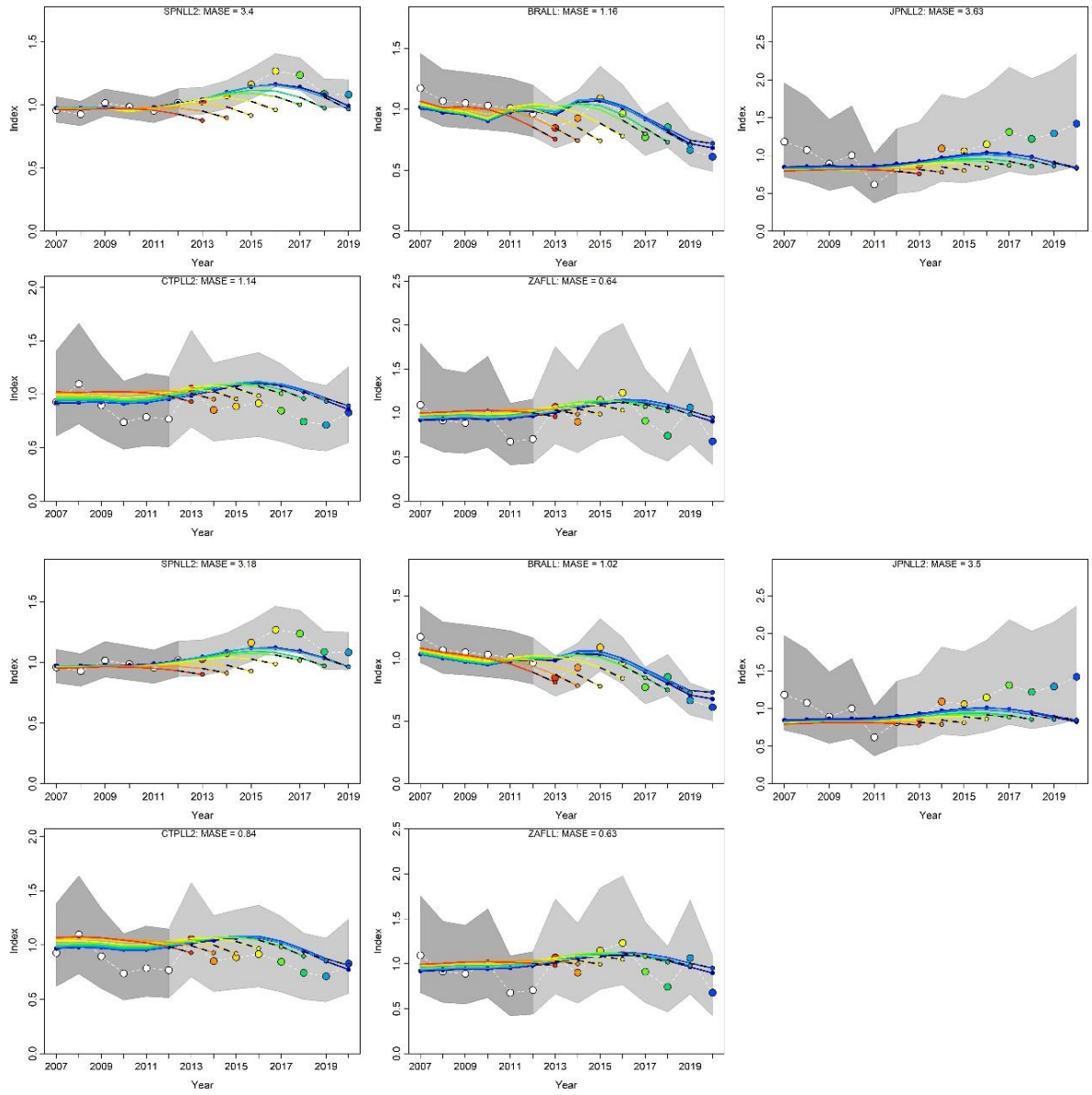

Figure 14. Hindcasting cross-validation results for the two SS3 models for the South Atlantic swordfish ("Sel_Asym_model" – upper panels and Sel_DN model – lower panels), showing one-year-ahead forecasts of CPUE values (2013-2020), performed with eight hindcast model runs relative to the expected CPUE. The CPUE observations, used for cross-validation, are highlighted as color-coded solid circles with associated light-grey shaded 95% confidence interval. The model reference year refers to the end points of each one-year-ahead forecast and the corresponding observation (i.e. year of peel + 1).

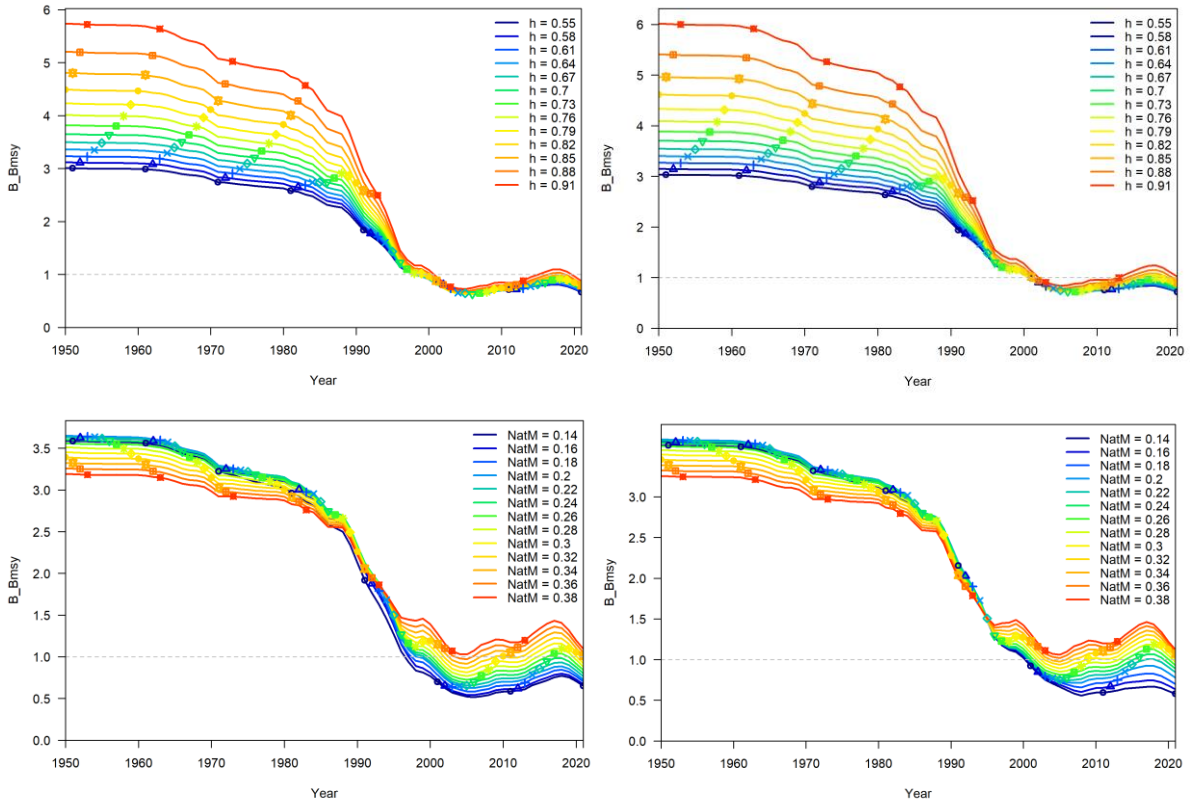

Figure 15. Sensitivity analysis performed for the alternative natural mortality (lower panels) and steepness (upper panels) from the base case model for the South Atlantic swordfish showing the time-series spawning biomass relative to SSB_{MSY} (SSB/SSB_{MSY}) and fishing mortality relative to F_{MSY} (F/F_{MSY}). Left panels ("Sel_Asym_model") and right panels ("Sel_DN model").

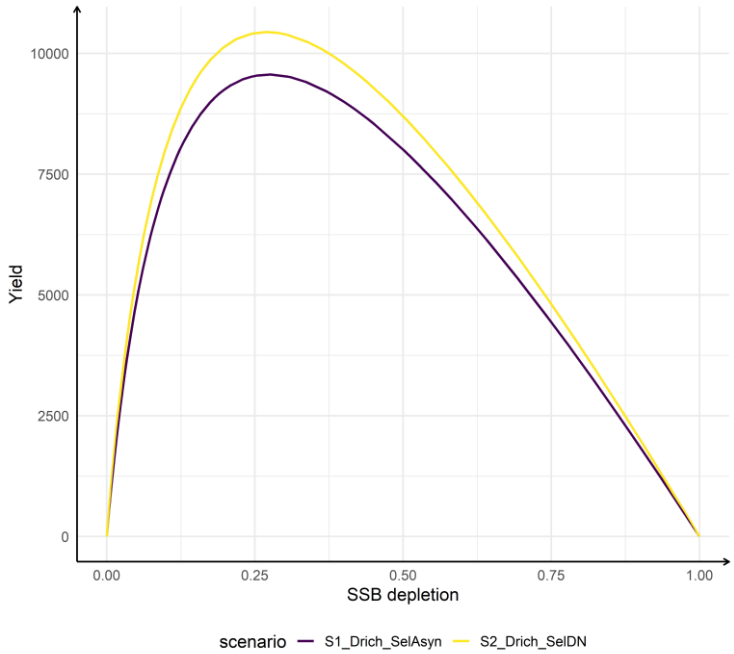

Figure 16. Yield curve by depletion levels of spawning biomass for the two SS3 models for the South Atlantic swordfish.

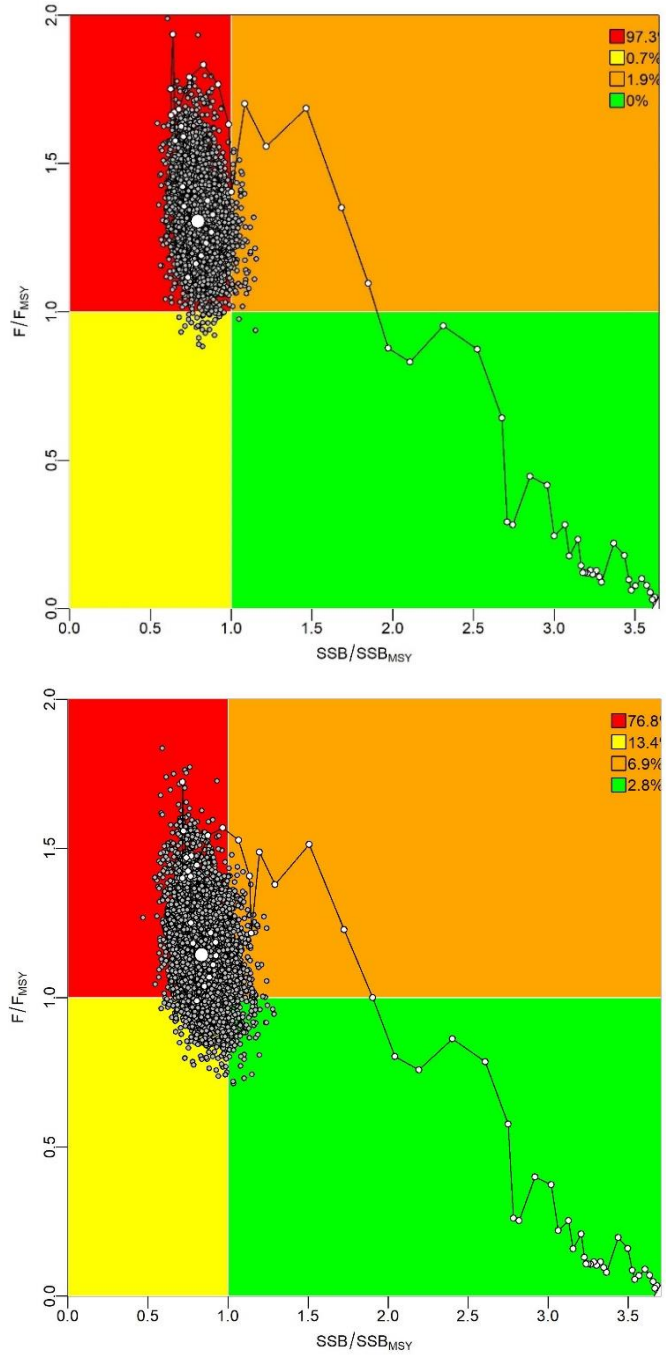

Figure 17. Kobe phase plot showing estimated trajectories (1950-2020) of SSB/SSB_{MSY} and F/F_{MSY} for the two SS3 models for the South Atlantic swordfish. The probability of terminal year points falling within each quadrant is indicated in the figure legend. Upper panels ("Sel_Asym_model") and lower panels ("Sel_DN model").